ADVANCED FUNCTIONAL MATERIALS
www.afm-journal.de

Model Organic Surfaces to Probe Marine Bacterial Adhesion Kinetics by Surface Plasmon Resonance

*Alice Pranzetti, Stéphanie Salaün, Sophie Mieszkin, Maureen E. Callow, James A. Callow, Jon A. Preece, and Paula M. Mendes**

Understanding how bacteria adhere to a surface is a critical step in the development of novel materials and coatings to prevent bacteria forming biofilms. Here, surface plasmon resonance (SPR) spectroscopy, in combination with self-assembled monolayers (SAMs) that have different backbone structures and/or functional groups, is used for the first time to study the initial stages of bacterial adhesion to surfaces (i.e., initial interaction of cells with a surface, a process governed by van der Waals, electrostatic, and hydrophobic interactions). The work highlights SPR spectroscopy as a powerful and unique approach to probe bacterial adhesion in real time. SPR spectral data reveal different kinetics of adhesion for the interaction of two marine bacterial species (*Marinobacter hydrocarbonoclasticus* and *Cobetia marina)* to a range of organosulfur SAMs. Furthermore, the extent of adhesion is dependent on the backbone structures and functional groups of the SAMs. The role of extracellular polymeric substances (EPS) in bacterial adhesion is also investigated. Pre-conditioning experiments with cell-free culture supernatants, containing planktonic EPS, allow quantification of the amount adsorbed onto surfaces and directly account for the impact of EPS adsorption on bacterial adhesion in the assay. While the physicochemical characteristics of the surfaces play a significant role in determining bacterial cell adhesion for low levels of conditioning by planktonic EPS, greater levels of conditioning by EPS reduce the difference between surfaces.

1. Introduction

Research on bacterial adhesion is a field covering areas such as marine science, soil and plant ecology, food safety, and the biomedical field.[1] As an integral part of their survival mechanism, bacteria have a natural tendency to adhere to surfaces. Surface-attached bacterial cells may develop into biofilms, which can have beneficial or adverse effects on such a surface, depending on whether their formation within a specific system is intentional or not.[1] For instance, bacterial biofilms are of great practical importance for technologies such as wastewater treatment and bioremediation of groundwater and soil. In other settings, long-term adhesion and the development of bacterial colonies or biofilms are responsible for biofouling in marine and industrial systems, a wide variety of microbial infections in the human body, and many other expensive and life-threatening situations.[2] As a result, knowledge of bacterial adhesion to surfaces is essential for promoting or preventing biofilm formation, as well as for understanding bacterial ecology.

Since the nature of the surface and the type of bacteria may dictate whether or not cells will adhere at an interface, efforts have been made to modify the interfacial properties to understand bacterial adhesion.[3,4] Such efforts have triggered the need for experimental approaches to quantify the adhesion of bacteria on artificial surfaces. To date, bacterial adhesion assays have been developed using enzyme-linked immunosorbent assay (ELISA),[5] radiolabeling,[6] plate counting,[7] and various types of staining, such as the use of nucleic acid–binding fluorochromes (e.g., SYTO 13),[8] or more general stains such as the Gram stain,[9] followed either by direct microscope counting (with or without image analysis) or by dye extraction,[10] or in the case of SYTO 13, by the direct use of a fluorescence plate reader.

Although useful and informative, these procedures present several limitations. Plate counting and evaluation after staining of the bacteria are time-consuming and tedious, and are therefore not suitable for high-throughput analyses (i.e., for testing numerous bacteria or assay conditions). Methods developed for high throughput screening require a high density of attached cells.[8,10] The radiolabeling assay is more accurate and simple, but the use of radioactive labels needs safety evaluation.[11] Large-scale experiments can be carried out using ELISA-based methods, but specific antibodies are not always readily available, and can be laborious or impossible to produce.[12] Furthermore, none of these techniques can provide information about the kinetics of adhesion, in real time. Noting these issues, there

A. Pranzetti, Dr. P. M. Mendes
School of Chemical Engineering
University of Birmingham
Edgbaston, Birmingham, B15 2TT, UK
E-mail: p.m.mendes@bham.ac.uk
A. Pranzetti, Prof. J. A. Preece
School of Chemistry
University of Birmingham
Edgbaston, Birmingham, B15 2TT, UK
Dr. S. Salaün, Dr. S. Mieszkin, Dr. M. E. Callow, Prof. J. A. Callow
School of Biosciences
University of Birmingham
Edgbaston, Birmingham, B15 2TT, UK

DOI: 10.1002/adfm.201103067

remains a need for antibody-free and label-free assays that enable real time monitoring of bacterial adhesion to surfaces without secondary agents.

Surface plasmon resonance (SPR) is a powerful optical technique that detects molecular interactions on a metal surface in real time in a label-free environment. It has been widely used for the quantification and kinetic analysis of receptor–ligand interactions,[13] but so far SPR has been of only limited[14] use in the analysis of bacterial interactions. Previous studies have mainly concentrated on the sensing performance (i.e., sensitivity and selectivity) of SPR to detect bacterial cells,[14] and detection limits as low as 10^2–10^6 cells/mL have been reported.[15] A few other studies have applied the SPR technique to discriminate between wild-type and mutant bacterial strains,[16] to analyze the affinity of bacteria for surface-immobilized host components, including proteins[17] and glycolipids,[18] and to evaluate the inhibitory potency of multivalent galabiose derivatives on bacterial adhesion.[19]

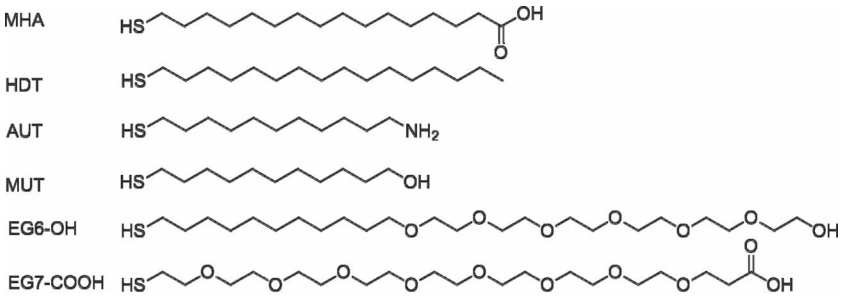

Figure 1. Chemical structures of the organosulfur compounds used for SAM preparation.

With its ability to monitor, in real time, interactions occurring in the vicinity of a metal surface (usually within 200 nm),[20] the SPR technique is advantageous for the investigation of the initial stages of bacterial adhesion at interfaces. The adhesion of bacteria to surfaces can occur through several mechanisms, including non-specific contributions from electrostatic, van der Waals, and hydrophobic forces,[21] and a variety of biospecific selective interactions (e.g., carbohydrate–protein, protein–protein).[4,22] Bacterial adhesion to surfaces varies from one bacterial species/strain to another, and also depends on the growth phase, thus adding to the complexity of the mechanisms through which bacteria attach to a surface.[3,4]

The physicochemical properties of a surface, including surface chemistry, charge, surface roughness, and wettability, are generally believed to be closely involved in regulating bacterial adhesion to a surface.[23] Nevertheless, many aspects of the competing mechanisms that regulate such adhesion remain unclear, in particular, those related to the role of extracellular polymeric substances (EPS) in the initial adhesion stage. The metabolic products of active bacterial secretions, consisting of a mixture of proteins, glycoproteins, polysaccharides, nucleic acids, and lipids are the constituents of EPS.[24] EPS are subdivided into "planktonic" or "bound", depending on whether the polymeric material is released into the surrounding medium or remains in close association with the bacterial cell surface.[24] Although it has been suggested that the presence of a layer of EPS on a surface facilitates, or is required for, the initial adhesion of bacteria,[25] this has been insufficiently examined to date. This partial examination is in part due to the lack of suitable tools that can quantify EPS adsorbed onto surfaces, from a solution and dynamically, and subsequently account for the impact of EPS adsorption on bacterial adhesion.[26]

Here, SPR provides label-free detection and real time observation of both EPS and bacterial adhesion to model organic surfaces to gain novel insights into how the physicochemical characteristics of the surface direct the adhesive nature of the bacteria. In particular, a SPR-based assay was developed to elucidate the role that EPS play in driving the first step of adhesion of bacteria to a surface. SPR-based assays were developed in a complex medium, namely artificial seawater (ASW), with two species of marine bacteria: *Marinobacter hydrocarbonoclasticus* and *Cobetia marina*. These bacteria were chosen because of their different hydrophobicities and EPS production characteristics. *C. marina* is a hydrophilic bacterium with a contact angle of 15.5°, whereas *M. hydrocarbonoclasticus* is a hydrophobic marine bacterium with a contact angle of 81.5°.[27] Furthermore, *C. marina* produces large quantities of exopolysaccharides, which are rich in uronic acids,[28] whereas the EPS of *M. hydrocarbonoclasticus* is more enriched in lipids than carbohydrates, as well as containing substantial proportions of waxy esters and sulfates.[29] Both species have been used as model bacteria to study the performance of putative antifouling coatings suitable for the marine environment.[27]

2. Results and Discussion

We chose to use self-assembled monolayers (SAMs) of organosulfur compounds on gold substrates as model organic surfaces because they allow molecular-level control of the properties of the surface. In this study, six different organosulfur SAMs on gold were investigated (**Figure 1**): 16-mercaptohexadecanoic acid (MHA), 1-hexadecanethiol (HDT), 11-aminoundecanethiol hydrochloride (AUT), 11-mercapto-1-undecanol (MUT), (11-mercaptoundecyl)hexa(ethylene glycol) (EG6-OH), and *O*-(2-carboxyethyl)-*O*′-(2-mercaptoethyl)heptaethylene glycol (EG7-COOH). The organosulfur compounds studied possessed not only different backbones (i.e., hydrophilic and hydrophobic), but also different terminal functional groups (hydrophilic, hydrophobic, positively charged, negatively charged, and neutral). For instance, the surface pK_a of MHA and AUT have been reported to be 7.9[30] and 7.5[31] (**Figure 2**), respectively, indicating that at pH 8.1–8.2 (i.e., pH of the ASW used in this study) the MHA SAM is partially deprotonated[30] (negatively charged) and AUT partially protonated[31] (positively charged). EG7-COOH SAM is expected to have a similar pK_a to MHA,[30] and thus it also carries a partial negative charge at the pH of the study. Concerning HDT, EG6-OH, and MUT, their pK_a values are too high (pK_a HDT > 35, pK_a EG6-OH and MUT ≥ 19–20[32]) to carry a charge at the pH of the ASW, and therefore, in this study, they will be considered as neutral SAMs.

SAMs of these compounds were prepared on gold surfaces and were characterized by contact angle measurement and

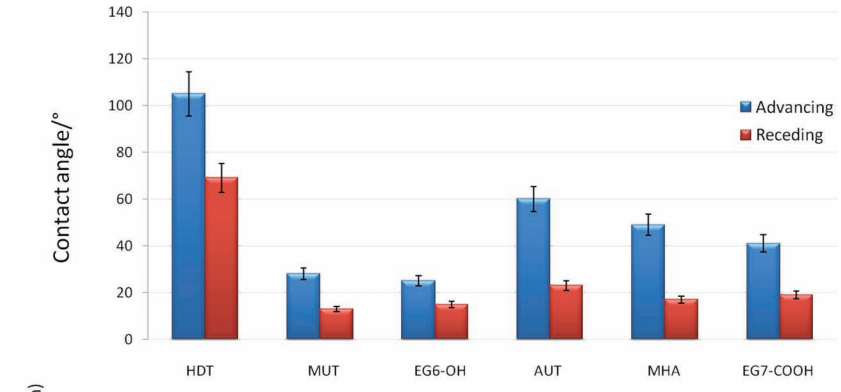

Thickness values (nm)	HDT	MUT	EG6-OH	AUT	MHA	EG7-COOH
Experimental[a]	1.73 ± 0.20	1.16 ± 0.18	2.97 ± 0.25	1.43 ± 0.23	1.65 ± 0.18	2.27 ± 0.19
Theoretical[b]	2.13	1.50	3.10	1.50	2.03	2.50
pK_a[c]	>35	~20	~20	7.5	7.9	~7.9

Figure 2. Advancing and receding water contact angles, ellipsometric thickness, and pK_a values for the different organosulfur SAMs. SAM abbreviations are defined in Figure 1. In the figure, (a) indicates the SAM thickness obtained from ellipsometry, (b) indicates the molecular length obtained from Chem 3D software, and (c) indicates the pKa obtained from literature data.

ellipsometry. The contact angle values obtained (Figure 2) were in good agreement with literature data.[33] EG6-OH and MUT had the lowest advancing contact angles (25° ± 3° and 28° ± 2°, respectively). The lowest contact angle of the carboxylic acid–terminated SAMs was found for the one containing a hydrophilic backbone (EG7-COOH, 41° ± 2°), with a slightly higher contact angle than the carboxylic acid–terminated SAM containing a hydrophobic backbone (MHA, 49° ± 2°). The advancing contact angle for the amino-terminated SAM (AUT, 60° ± 2°) was higher, in accordance with the lower surface energy reported for this surface.[34] The highest advancing contact angle was observed for HDT SAM (105° ± 4°) as a result of the higher hydrophobicity of both the backbone and the end group. Thickness of the SAMs was measured by ellipsometry, and the values reported in Figure 2 were in agreement with the theoretical calculations (Chem 3D Software) and literature data for similar monolayers.[35]

Following characterization of the SAMs, SPR was used to investigate the initial stages of bacterial adhesion as a function of SAM type (i.e., with differences in charge, wettability, and packing of the SAMs) by performing three different bacterial adhesion assays, SPR assays 1a, 1b, and 2 in **Figure 3**. In SPR assay 1 (Figure 3), the organosulfur SAMs on gold were exposed either to the EPS solution (SPR assay 1a) obtained by filtration of the two bacterial suspensions or to the bacterial suspensions (SPR assay 1b). Initial SPR studies were performed by exposing the SAMs to freshly prepared bacterial suspension (SPR assay 1b; ageing time = 0 min, T0). The organosulfur SAMs on gold were exposed to a flow of ASW, to establish the baseline, followed by an injection of bacteria in ASW at an OD_{600} = 1 (i.e., unity optical density at a wavelength of 600 nm) into the SPR flow cell at the rate of 25 µL min^{-1}, for 25 min. The SPR flow cell was then flushed with ASW to leave only the irreversibly adhered bacteria on the SAM. The amount of bacterial adhesion is defined as the difference in the SPR response units between the beginning of injection of bacteria and the end of washing with ASW. It can be inferred from the curves (**Figure 4**a,b, SPR assay 1b) that the amount of bacterial adhesion for both species is dependent upon the physicochemical nature of the surfaces.

The results suggest that electrostatic interactions play an important role in the initial bacterial adhesion process. Bacteria attached preferentially to charged surfaces (negative: EG7-COOH and MHA; positive: AUT) rather than neutral surfaces (HDT, EG6-OH, MUT). However, internal hydrophilicity and a lower packing density[36] significantly favored resistance to bacterial adhesion. For instance, negatively charged SAMs with an oligo(ethylene glycol) interior (EG7-COOH) showed higher resistance to adhesion of both *M. hydrocarbonoclasticus* and *C. marina* than negatively charged SAMs with a reported high packing density[37] and hydrophobic backbone (MHA). On the other hand, SPR data showed that the overall hydrophobicity of the SAMs appears not to influence appreciably the adhesion process of both bacterial species since the HDT (most hydrophobic SAM) and the EG6-OH (one of the most hydrophilic surfaces) SAMs are the most antifouling surfaces.

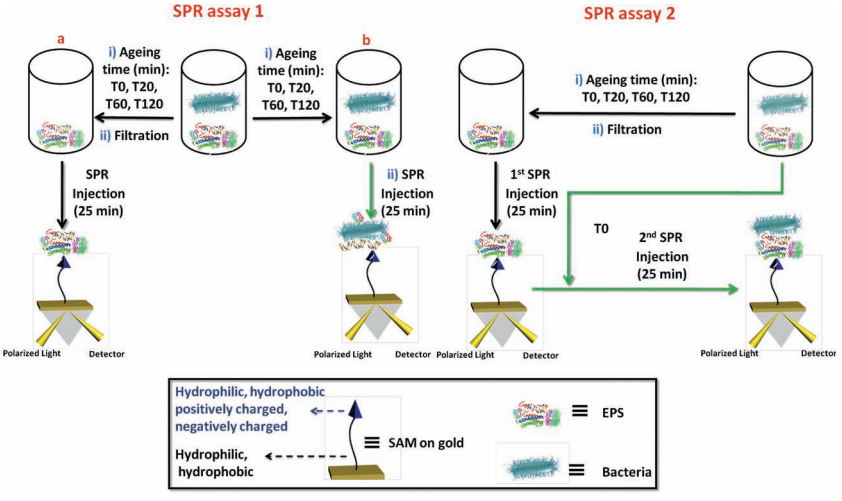

Figure 3. Schematic showing the bacterial adhesion assays performed using SPR. SPR assay 1: Organosulfur SAMs on gold were either a) exposed to soluble EPS solutions collected after different ageing times, T0–T120, or b) exposed to the two marine bacterial species collected after different ageing times, T0–T120. SPR assay 2: Organosulfur SAMs on gold were exposed to soluble EPS solutions collected after different ageing times, T0–T120 (1st SPR injection) prior to exposure to a freshly prepared bacterial suspension (T0) (2nd SPR injection). Soluble EPS was collected by filtration from bacterial suspensions after 0 (T0), 20 (T20), 60 (T60), and 120 (T120) min of bacterial ageing in ASW.

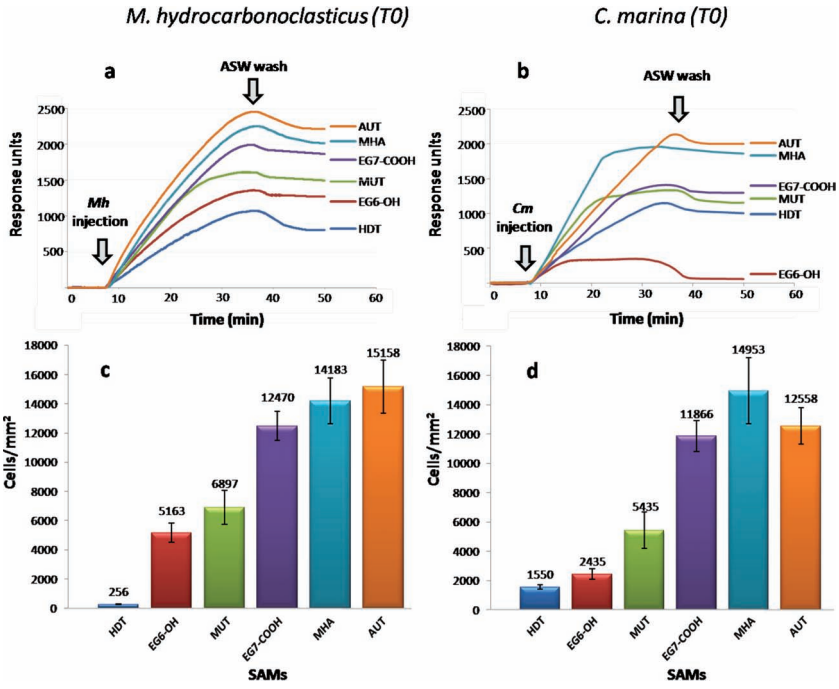

Figure 4. a,b) Sensorgram traces obtained from the SPR *M. hydrocarbonoclasticus* (*Mh*; a) and *C. marina* (*Cm*; b) adhesion assays (SPR assay 1b; ageing time = 0 min, T0) performed on SAMs of the indicated organosulfur compounds (abbreviations are defined in Figure 1). c,d) Number of *M. hydrocarbonoclasticus* (*Mh*; c) and *C. marina* (*Cm*; d) bacteria that adhered per square millimeter of the surface of the SAMs formed with the indicated organosulfur compound using a 60 min standard bacterial adhesion assay. The error bars are ± the standard deviation.

For each surface, SPR-assay experiments were performed in triplicate and similar SPR curves and final responses were obtained (Figure S1 in the Supporting Information) demonstrating the reproducibility of our SPR-based assays. Zeta potential studies were carried out in ASW in order to establish the charge on the bacteria. Both species of bacteria were found to be negatively charged (*C. marina*: –33.1 ± 0.3 mV; *M. hydrocarbonoclasticus*: –15.9 ± 0.5 mV; Figure S2 in the Supporting Information), which may explain the highest adhesion of both species of bacteria to the partially positively charged SAM, AUT. However, the presence of positive domains[38] on the external membrane of the bacteria could also explain the high adhesion to negatively charged SAMs (i.e., MHA). Furthermore, bacteria with hydrophobic characteristics (*M. hydrocarbonoclasticus*) showed the lowest adhesion on the most hydrophobic surface (HDT) and those with hydrophilic characteristics (*C. marina*) adhered to the lowest extent on the most hydrophilic surface (EG6-OH). In a previous report, *C. marina* showed a similar trend to the one obtained in this study whereas *M. hydrocarbonoclasticus* exhibited an opposite effect by preferring hydrophobic surfaces.[39] In this earlier report, the surfaces were based on poly(dimethylsiloxane) (PDMS) coatings (hydrophobic surfaces) and PDMS treated with plasma (hydrophilic surfaces).[39] In another study employing galactoside-terminated alkanethiol SAMs, both *C. marina* and *M. hydrocarbonoclasticus* preferentially adhered to the most hydrophilic SAMs.[40] The observed inconsistent patterns between bacterial adhesion and wettability suggest that the effect of the hydrophobicity of bacteria on bacterial adhesion to a surface is determined not only by surface wettability, but also by the backbone and terminal functional groups and its surface density. This suggestion is also in line with the observation that SAMs with similar wettabilities (EG6-OH and MUT) but different backbone structures and packing density led to considerably different bacterial adhesion (Figure 4). These findings are also in agreement with previous publications, in which protein[41] and algal cell[42] adhesion was found to be dependent on the internal and terminal hydrophilicity and packing density of the SAM. However, in these studies protein- and algal-adhesion resistance was favored by both internal and terminal hydrophilicity of the SAMs. Although such studies showed a correlation between the adsorption of proteins and cell adhesion on SAMs, other studies found little or no evidence to support the generalization that SAMs exhibiting optimal protein-resistance properties are also ideal candidates to prevent bacterial and mammalian cell adhesion.[40,43]

Subsequent to the SPR analysis, the colonized gold surfaces were chemically fixed with glutaraldehyde, stained with SYTO13, and examined by epifluorescence microscopy. The images (Figure S3 in the Supporting Information) qualitatively demonstrate the similarities in the colonization by the two species of bacteria on the various modified gold surfaces, which are in agreement with the SPR spectral data (i.e., neutral SAMs have relatively little bacterial adhesion while the charged SAMs have more bacterial adhesion). In addition, standard 60 min adhesion assays, using SYTO13 staining followed by direct cell counting by image analysis, were performed to quantify and validate the reliability of the SPR in the evaluation of bacterial adhesion. Standard end-point assays showed similar patterns for the adhesion of both species of bacteria (Figure 4c,d) on the six different surfaces, with neutral surfaces (HDT, EG6-OH and MUT) showing the lowest bacterial adhesion, while the charged surfaces had the highest density of attached bacteria. Note that the difference in trend between the SPR assay and end-point assay observed for HDT and EG6-OH SAMs using *C. marina* may be related to the flow-induced shear stress applied during the SPR assay 1b, which is not present in the standard assay. In contrast with other SAMs, *C. marina* was found to adhere weakly to the EG6-OH SAMs, since cells were easily washed away in the rinsing process, indicating that flow-induced shear stress may play a role in preventing attachment or washing off already bound bacteria on EG6-OH SAMs. Despite the use of different conditions in the two assays (i.e., SPR assay: OD_{600} = 1, time of adhesion = 25 min, and continuous flow-induced shear stress; standard assay: OD_{600} = 0.1, time of adhesion = 1 h, and shaking-induced shear stress), the overall high degree of correlation was reassuring and indicated that the two assays generate similar results. These results demonstrate that SPR can be used as a reliable and rapid assay to evaluate initial

stages of bacterial adhesion. Furthermore, compared with the standard adhesion assays, the SPR assay has the advantage of monitoring the adhesion of bacteria on surfaces in real time, thus allowing the interpretation of kinetic information on bacterial adhesion and interaction mechanisms.

Measurement of the attachment of *M. hydrocarbonoclasticus* by SPR gave a characteristic series of similar curves (Figure 4a), differing only in the rate at which bacterial adhesion occurs on the different surfaces. A higher rate of bacterial adhesion was observed for surfaces that can interact electrostatically with bacteria (EG7-COOH, MHA, and AUT), in contrast to the neutrally charged surfaces (HDT, EG6-OH, MUT). Indeed, during the 25 min time frame of the flow of bacteria over the charged SAMs (AUT, MHA, EG7-COOH), the response units did not reach the plateau. Upon washing of all the surfaces with ASW there was a small drop in the SPR response, indicating that most of the bacteria were well adhered. We believe that the increase in the SPR response is due solely to bacterial deposition on the surface and not to cell division, as the cell suspension concentration remained constant over 120 min in the ASW minimal medium and microscopy observation revealed no division of cells on the surfaces.

Although no substantial differences in the relative density of adhered cells (Figure 4c,d) between the two species of bacteria on the various SAMs could be detected in standard end-point adhesion assays (with the exception of HDT and EG6-OH for *C. marina*), clear differences in the kinetics of bacterial adhesion were observed by SPR. For *M. hydrocarbonoclasticus* the surfaces that exhibited the fastest rate of adhesion had the highest bacterial adhesion upon washing (Figure 4a). However, for *C. marina* this direct relationship between rate of adhesion and final bacterial adhesion was not observed (Figure 4b). For instance, although MUT and MHA SAMs exhibited faster rates of adhesion than AUT SAMs, the AUT SAMs showed the highest final number of adhered *C. marina* cells. Actually, the shape of the SPR curve for *C. marina* (Figure 4b) was dependent upon the surface analyzed, with some SPR sensorgrams saturating after 8–12 min (EG6-OH, MUT, and MHA) of exposure to bacteria. Bacterial equilibrium adhesion values were dependent on the chemical properties of the SAM. The lowest number of cells of *C. marina* adhering at equilibrium was found with EG6-OH SAMs. When ASW replaced the cell suspension, the SPR signal dropped back close to baseline levels, which suggests that on EG6-OH surfaces most bacteria adhered weakly, and were easily washed away. It is interesting to note the significance of the oligo(ethylene glycol) backbone of the EG6-OH SAM in reducing the degree of adhesion, since a SAM with a similar end group but with a hydrophobic backbone (MUT) gave intermediate final numbers of adhering bacteria (Figure 4b). The maximum final number of adhered cells of *C. marina* was obtained with charged SAMs with hydrophobic backbones (MHA and AUT; Figure 4b). These data show not only that the end group of the SAM is critical in influencing initial attachment, but also that the backbone functionality influences the strength of adhesion.

The SPR signals obtained in these experiments will be composed of contributions not only from the binding of the cells, but also from the physisorption of EPS, either present in the experimental cultures at time zero and/or secreted by the bacteria during the period of measurements (up to 40 min). To analyze the influence of EPS on the SPR signal, SPR assays 1a and 1b (Figure 3) were performed. SPR assays 1a were carried out using cell-free supernatant (EPS) derived from filtered bacterial cultures aged in ASW for 0–120 min. The suspensions of *C. marina* and *M. hydrocarbonoclasticus* were filtered through a 0.22 μm membrane filter after 0 (T0), 20 (T20), 60 (T60), and 120 (T120) min ageing in ASW. The resulting EPS-containing supernatants were introduced into the SPR flow cell at a flow rate of 25 μL min^{-1} for 25 min, after which the surfaces were rinsed with ASW. Overall SPR sensorgrams demonstrated (**Figure 5**a) that EPS adsorbed in higher amounts with longer times of cell ageing (T60–T120). For instance, HDT SAMs exposed to a solution of cell-free, EPS-containing supernatant of *C. marina* prepared at T0 showed only a small SPR response (~100 response units), but this response was progressively greater for supernatants collected at T20, T60, and T120. Evidence of the dependence of the SPR responses on the EPS concentration was demonstrated by challenging HDT SAMs

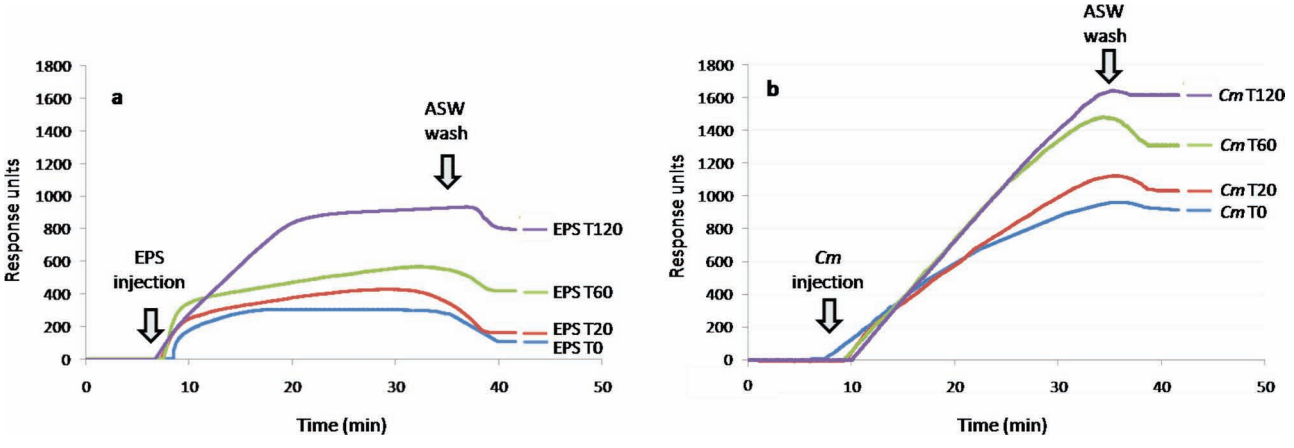

Figure 5. Sensorgram traces obtained from the adhesion of a) EPS on HDT SAMs collected by filtration at 0 (T0), 20 (T20), 60 (T60), and 120 (T120) min of *C. marina* bacterial suspension ageing time (SPR assay 1a) and b) *C. marina* (Cm) on HDT SAMs at 0 (T0), 20 (T20), 60 (T60) and 120 (T120) min of bacterial suspension ageing time (SPR assay 1b).

with a range of EPS dilutions. An undiluted EPS solution collected from a *C. marina* culture aged in ASW for 180 min and EPS solutions diluted with ASW to 25, 50, 60, 65, 75, 80, and 100% (v/v) were introduced into the SPR flow cell at a flow rate of 25 µL min^{-1} for 25 min, after which the surfaces were rinsed with ASW. The SPR response decreases linearly with increasing dilution of EPS (Figure S4 in the Supporting Information), confirming that the higher SPR responses in Figure 5a are due to the higher concentrations of EPS in the injected solution.

SPR assays 1b (Figure 3) were conducted with both species of marine bacteria using a freshly prepared bacterial suspension (T0), and cells aged for 20 (T20), 60 (T60), and 120 (T120) min in ASW. The SPR baseline for the SAM-modified gold chips was established using ASW, following which the bacterial suspensions in ASW at an OD_{600} = 1 were introduced into the SPR flow cell at the rate of 25 µL min^{-1} (Figure 5b). Data were collected for 25 min, followed by washing with ASW. In general, the results showed that cells aged for longer times displayed higher SPR responses. For instance, for the HDT SAM exposed to a suspension of *C. marina* aged for 120 min in ASW, the SPR signal increased by ~700 response units (Figure 5b). Since the cells did not divide in ASW up to T120, these results suggest that the higher SPR response with cells aged in the minimal medium (ASW) was due to an increased physisorption of EPS progressively secreted by the bacteria with time. Comparison of Figure 5a,b enables an estimate of the relative contributions of EPS and cells to the SPR signal. On the HDT SAM for example, after the SPR sensor chip was rinsed with ASW, the residual signal for the T0 cell-free supernatant was ~100 response units (Figure 5a) and for the freshly prepared bacterial suspension (T0) ~1000 response units, indicating that EPS contributes to ca. 10% of the signal for the complete culture. This rose to ca. 50% for cells that had been aged for 120 min.

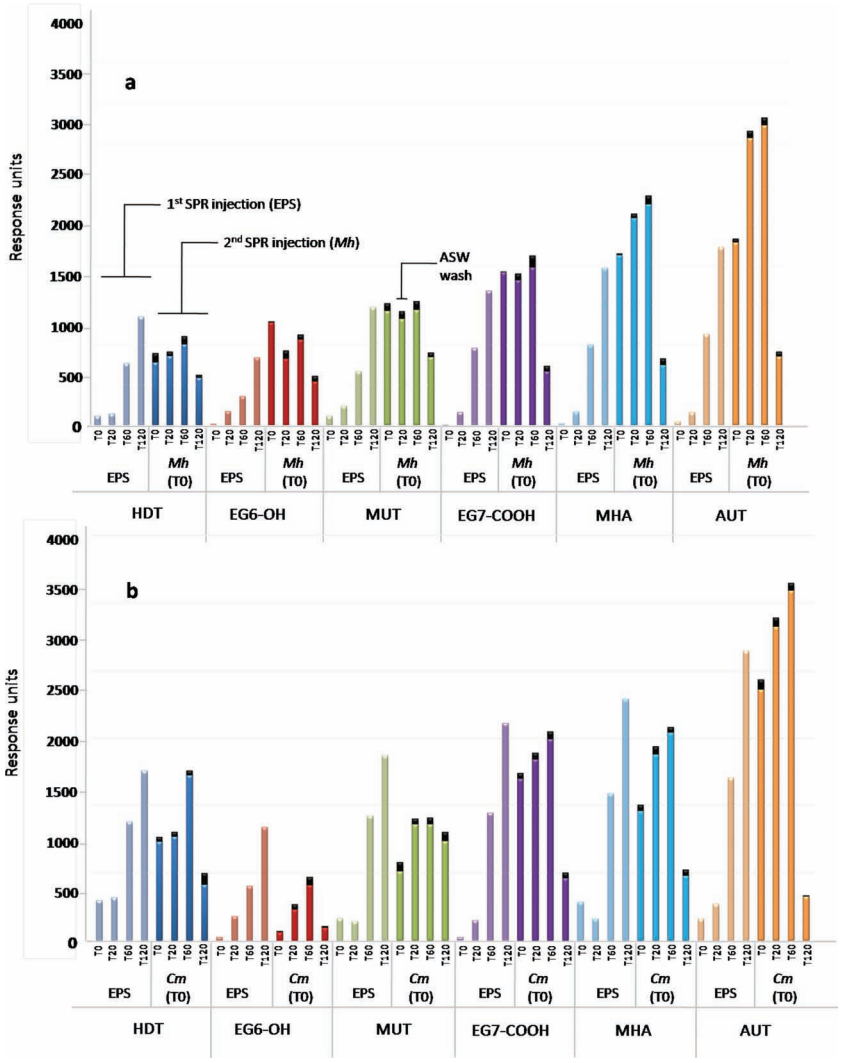

Figure 6. SPR responses to bacteria a) *M. hydrocarbonoclasticus* (*Mh*) and b) *C. marina* (*Cm*) following pre-conditioning of a range of organosulfur SAMs with cell-free, EPS-containing culture filtrates. The gold-coated SPR chips derivatized with SAMs were pre-conditioned for 25 min with cell-free culture filtrates (EPS) collected from bacteria aged in ASW for 0 (T0), 20 (T20), 60 (T60), and 120 (T120) min (SPR Assay 2,1st SPR Injection). The SPR signal after 25 min is shown on the histogram as EPS T0, T20, T60, and T120. The pre-conditioned chips were then incubated, under flow, with fresh bacterial suspensions for 25 min and washed (SPR Assay 2, 2nd SPR Injection). The drop in the SPR response units related to the washing step is indicated by the black segments in the histogram. The amount of bacterial adhesion shown on the histogram as *Mh* (or *Cm*) T0 was determined by the difference between the signal at the injection of the bacteria and the signal after washing (see Figure S5 in the Supporting Information).

In an effort to further delineate the effects of surface conditioning by EPS on adhesion of bacteria, SPR assay 2 was carried out by pre-conditioning the SAMs with EPS-containing bacteria-free filtrates collected from cells aged in ASW for 0 (T0), 20 (T20), 60 (T60), and 120 (T120) min (SPR assay 2, first SPR injection, Figure 3). The resulting surfaces were then immediately challenged (SPR assay 2, second SPR injection, Figure 3) with freshly prepared bacterial suspensions (OD_{600} = 1). As before, the baseline for the SAM-modified gold chip was established using ASW, following which the bacteria-free filtrate (EPS T0, T20, T60, and T120) was introduced at a flow rate of 25 µL min^{-1}. Data were collected for 25 min, under continuous flow, after which a freshly prepared bacterial suspension, *M. hydrocarbonoclasticus* or *C. marina* (EPS T0) in ASW (OD_{600} = 1), was introduced into the SPR flow cell at the rate of 25 µL min^{-1}. The sensor chip was not rinsed with ASW between the two injections. The flow of bacteria was carried out for a further 25 min, after which the SPR flow cell was flushed with ASW to remove any loosely bound or unbound bacteria.

The SPR responses obtained following subsequent EPS pre-conditioning (SPR assay 2, first injection) and exposure to bacterial suspensions (SPR assay 2, second injection) are illustrated in **Figure 6**a (*M. hydrocarbonoclasticus*) and 6b (*C. marina*). For each SAM, two sets of response signals are obtained for T0,

T20, T60, and T120. The first set of responses, labeled "EPS" in the graphs, corresponds to the difference in the SPR response units between the beginning and end of injection of EPS collected from cells aged in ASW for 0 (T0), 20 (T20), 60 (T60), and 120 (T120) min (SPR assay 2, first injection). Following pre-conditioning of the SAM with these EPS-containing culture filtrates (EPS T0–T120), the second set of responses, named either "*Mh* (T0)" or "*Cm* (T0)", corresponds to the difference in the SPR response units between the beginning of injection of freshly prepared bacterial suspension, *M. hydrocarbonoclasticus* and *C. marina* (T0), and the end of washing with ASW (SPR assay 2, second injection). The drop in the SPR response units related to the washing step is indicated by the black segment in the histograms of the second set of responses named either "*Mh* (T0)" or "*Cm* (T0)" (Figure 6). An example of a SPR sensorgram, together with an illustration of how the response signals were obtained, is provided in Figure S5 (Supporting Information).

Considering first the response signals to the pre-conditioning EPS treatments ("EPS" in Figure 6a,b), we see that longer periods of ageing of the bacterial suspension from which the EPS was derived progressively increased the signal, presumably owing to higher concentrations of EPS. For instance, while EPS binding was almost negligible for all the SAMs studied at EPS T0, SPR responses as high as 2000 response units were obtained if EPS was collected from bacteria aged for 120 min (EPS 120) in ASW (e.g., AUT SAM). It is noteworthy that for EPS collected at T0 and T20, the comparative resistance of the different surfaces to EPS adsorption did not correlate with their comparative resistance to adhesion of bacterial cells. However, for longer ageing times (EPS T60–EPS T120) the trend of EPS adsorption was similar to that observed for bacterial cell adhesion. In other words, for EPS collected at T60 and EPS T120, charge seems to play a dominant role, rather than surface hydrophilicity.

Considering now the response of bacteria to the pre-conditioned surfaces ("*Mh* (T0)" or "*Cm* (T0)" in Figure 6a,b), we see that the extent of pre-conditioning influenced the subsequent extent of bacterial adhesion. It is important to note that rinsing did not cause any significant drop in the SPR response, indicating that the bacteria are retained on the SAM-modified surfaces with EPS and not washed off by rinsing. In general, the results showed a promoting effect on bacterial adhesion for surfaces preconditioned with EPS collected from cells aged in ASW for between 0 and 60 min. For instance, the charged surfaces, in particular MHA and AUT, showed an increase of *C. marina* adhesion when pre-conditioned with EPS obtained from bacteria aged in ASW for 0–60 min. *M. hydrocarbonoclasticus* showed a similar trend with the exception of EG7-COOH. The difference in trend observed for EG7-COOH might be due to the presence of an oligo(ethylene glycol) backbone, which could affect the packing of the SAM, and thus its adhesion properties. The responses obtained by exposure of the fresh bacterial suspension to pre-conditioned MHA and AUT SAMs showed a clear increase in the amount of bacteria adhering to the surfaces, with over 1000 response units for *M. hydrocarbonoclasticus* on the AUT SAM. For both species of bacteria, the increase in adhesion is less pronounced at T60 than at T20 on the charged surfaces. Overall the responses obtained for *C. marina* adhesion on the six SAMs were lower than for *M. hydrocarbonoclasticus*, indicating that the EPS effect is dependent on the species of bacteria.

Compared with charged SAMs, bacterial adhesion was not substantially affected on all neutral SAMs (HDT, EG6-OH, and MUT) pre-conditioned with bacterial supernatants (EPS) obtained from bacterial suspension aged in ASW for 0–60 min. Despite a substantial increase in the amount of EPS attached to these neutral surfaces for longer ageing times (EPS T20–T60), the quantity of bacteria detected by SPR did not change drastically for either species of bacteria. For these neutral surfaces, a small promoting effect on bacterial adhesion was observed between pre-conditioning the surfaces with EPS collected from cells aged in ASW for T20 and T60 min. In particular, comparing the amount of *M. hydrocarbonoclasticus* and *C. marina* (Figure 6a,b) attached to the neutral surfaces, a maximum difference of 500 response units was observed for HDT and EG6-OH SAMs. Also, the adhesion preferences of *M. hydrocarbonoclasticus* and *C. marina* noted in the previous experiments (Figure 4a,b) were maintained. These results suggest that for the levels of conditioning achieved with EPS collected from cells aged in ASW for 0, 20, and 60 min, the physicochemical characteristics of the surfaces played a significant role in determining bacterial cell adhesion.

Pre-conditioning with EPS from bacteria aged for 120 min, and therefore containing higher levels of EPS, substantially reduced the subsequent adhesion of bacteria and the trends in surface preference were less distinct. Since the difference in SPR signal before and after the ASW rinse was minimal for all the surfaces, the reduced bacterial adhesion may be due to phenotypic changes that occur in the cells when left in a minimal medium (ASW) for 120 min, including changes in EPS composition and properties. In order to establish whether the SPR responses accurately reflected cell adhesion, the pre-conditioned AUT SAMs challenged with *M. hydrocarbonoclasticus* and *C. marina* were visualized by epifluorescence microscopy and cell counting was performed. The density of bacteria for both *M. hydrocarbonoclasticus* (**Figure 7**) and *C. marina* (data not shown) was in agreement with the trends obtained from the SPR sensorgrams (Figure 6a).

3. Conclusions

Here, SPR has been employed as a reliable and rapid tool to evaluate initial stages of bacterial adhesion. The specific contributions of charge and wettability to bacterial adhesion were elucidated by employing SAMs with different characteristics. These studies have shown that electrostatic interactions play an important role in the initial bacterial adhesion process of both species of bacteria studied. In comparison with a standard adhesion assay, the SPR assay has the advantage of monitoring the adhesion of bacteria and other analytes on surfaces in real time, giving insights into the kinetics of adhesion. Since marine bacteria were used in our assays, we also showed that SPR is a suitable technique for work with complex media such as ASW, which contains a number of different electrolytes at pH 8.1–8.2. Furthermore, we were able to demonstrate that SPR is able to discriminate between signals derived from different

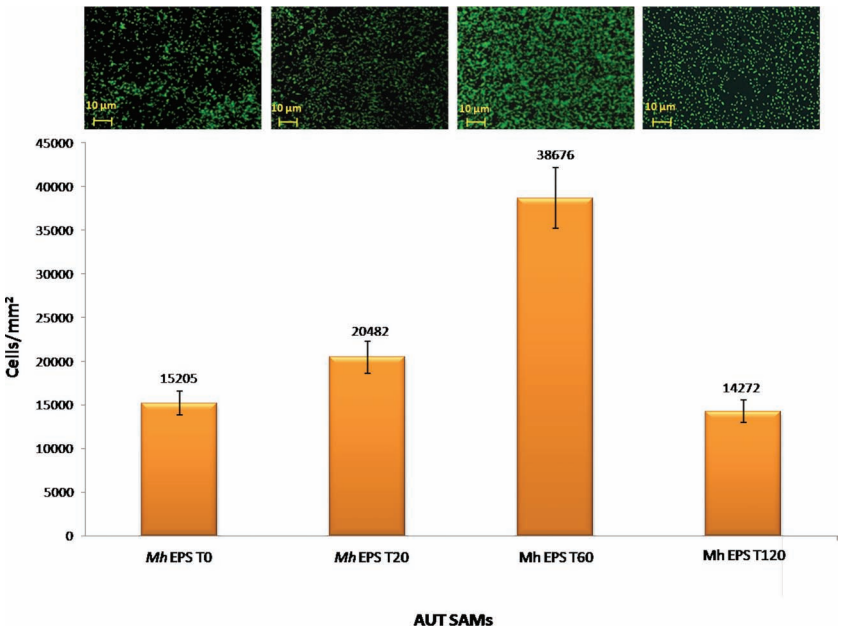

Figure 7. Fluorescence images of gold-coated SPR chips derivatized with AUT SAMs after the SPR-based AUT SAM-EPS-bacteria assays on *M. hydrocarbonoclasticus* (*Mh*) were performed as described in Figure 6. Below are shown the corresponding number of cells of *M. hydrocarbonoclasticus* (*Mh*) that adhered per square millimeter of the surface of the SAM-EPS conditioning film.

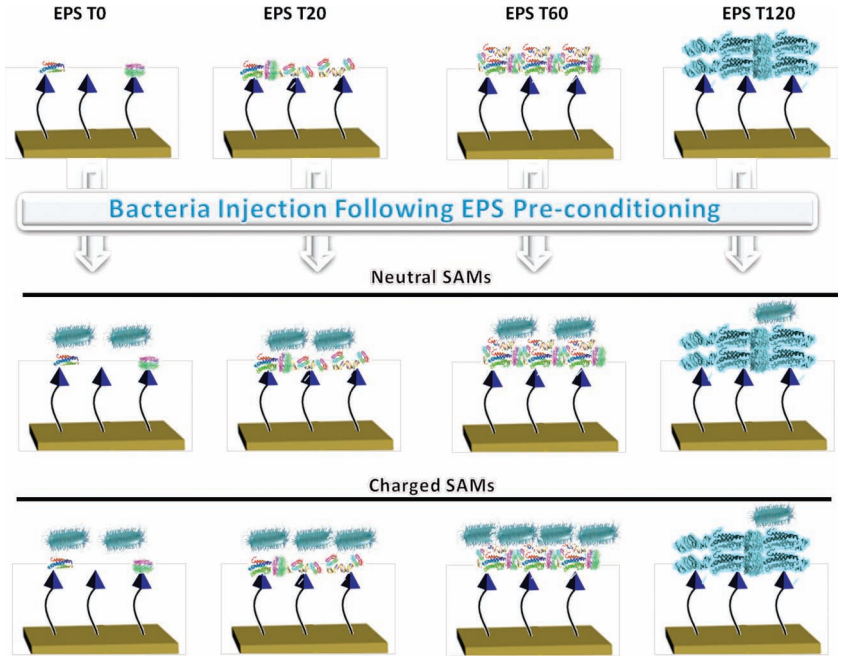

Figure 8. Schematic showing that higher amounts of EPS are adsorbed on the SAMs exposed to EPS derived from longer periods of ageing of the bacterial suspension, presumably owing to higher amounts of EPS secreted with time. This behavior is independent of SAM type (i.e., with differences in charge, wettability, and packing). Following EPS pre-conditioning, the enhancement in bacterial adhesion is more pronounced in charged than in neutral SAMs. However, for both bacterial species a threshold effect was observed in that bacterial adhesion was inhibited substantially by pre-conditioning the SAM surfaces with EPS from bacteria aged for 120 min, possibly owing to changes in the EPS properties for longer periods of cell ageing.

analytes, such as EPS and whole cells such as bacteria, allowing us to describe in some detail the effect of EPS on bacterial adhesion in a single assay. These single assays demonstrated that in circumstances where the level of conditioning of surfaces by EPS is likely to be small, this facilitates the initial adhesion of bacteria. However, the enhancement in bacterial adhesion is more pronounced on charged than in neutral SAMs, suggesting that, for such levels of EPS conditioning, the physicochemical characteristics of the surfaces strongly influence bacterial adhesion (**Figure 8**). On the other hand, greater levels of conditioning by EPS diminished the influence of the original surface properties. For both bacterial species studied, with the present experimental approach, the time at which the bacterial adhesion starts to become independent of the underlying surface properties is approximately 120 min of EPS secretion.

4. Experimental Section

SAM Preparation: Gold-coated (50 nm) Reichert sensor chips were rinsed with high-performance liquid chromatography ethanol (HPLC EtOH) and ultra high purity (UHP) H_2O (resistivity = 18 MΩ cm), exposed to UV light for 1 h, and rinsed with HPLC EtOH prior to use. 1-Hexadecanethiol (HDT, 99%), 16-mercaptohexadecanoic acid (MHA, 99%), 11-aminoundecanethiol hydrochloride (AUT, 99%), 11-mercapto-1-undecanol (MUT, 99%), O-(2-Carboxyethyl)-O′-(2-mercaptoethyl)heptaethylene glycol (EG7-COOH, 95%), (11-mercaptoundecyl) hexa(ethylene glycol) (EG6-OH, 90%), HPLC EtOH, triethylamine ($N(CH_2CH_3)_3$, 99.5%), trifluoroacetic acid (CF_3COOH, 99%) were purchased from Sigma-Aldrich (UK). SAMs were formed by immersing precleaned gold-coated substrates into a 1 mM solution of HDT, MHA, AUT, MUT, EG7-COOH, or EG6-OH in ETOH for 24 h at room temperature. Upon removal from the solution, the substrates were rinsed with HPLC EtOH and dried with a stream of N_2. Note that, on one hand, the NH_2-terminated SAMs were deposited in the presence of HPLC EtOH containing 3% (v/v) $N(CH_2CH_3)_3$ to prevent the formation of hydrogen bonds between the NH_2 functional groups of the bound thiol on the Au surface and that of free thiol in the bulk solution.[44] Upon SAM formation, the NH_2-terminated SAMs were rinsed in the presence of an ethanolic solution containing 10% (v/v) CF_3COOH. On the other hand, COOH-terminated SAMs were formed in the presence of HPLC EtOH containing 3% (v/v) CF_3COOH and then rinsed with an ethanolic solution of $N(CH_2CH_3)_3$ in order to prevent hydrogen bonds between COOH-terminated bound thiols and COOH-terminated thiols in solution.

Contact Angle Measurements: Contact angles were determined using a home-built contact angle apparatus, equipped with a charged coupled device

(CCD) KP-M1E/K camera (Hitachi) that was attached to a personal computer for video capture. The dynamic contact angles were recorded as a microsyringe was used to quasi-statically add liquid to or remove liquid from the drop. The drop was shown as a live video image on the PC screen and the acquisition rate was 4 frames per second. FTA video analysis software v1.96 (First Ten Angstroms) was used for the analysis of the contact angle of a droplet of UHP H_2O at the three-phase intersection. The averages and standard errors of contact angles were determined from five different measurements made for each type of SAM.

Ellipsometry: The thickness of the deposited monolayers was determined by spectroscopic ellipsometry. A Jobin-Yvon UVISEL ellipsometer with a xenon light source was used for the measurements. The angle of incidence was fixed at 70°. A wavelength range of 280–820 nm was used. DeltaPsi software was employed to determine the thickness values and the calculations were based on a three-phase ambient/SAM/Au model, in which the SAM was assumed to be isotropic and assigned a refractive index of 1.50. The thickness reported is the average of six measurements taken on each SAM. The errors reported for the ellipsometry measurements are standard errors.

Zeta Potential Measurement: Measurements of the overall surface charge of the bacterial cells in ASW were performed with a Malvern Instruments Zetasizer 4, using the ZET 5104 cell. The tests were performed at 25 °C and the measurement of each bacterial species was performed a total of three times.

Marine Bacterial Strains and Growth Conditions: *Cobetia marina* ATCC 25374$^{T[45]}$ and *Marinobacter hydrocarbonoclasticus* ATCC 49840$^{T[45]}$ (DSMZ, Germany) were revived from the original lyophilate and stored as frozen stock aliquots in liquid ZoBell medium [5 g of bacteriological peptone (Oxoid) and 1 g of yeast extract (Merck) in 800 mL ASW filtered through 0.22 µm membrane filters (500 mL bottle top filter, Corning Incorporated) and 200 mL deionized water] + 20% glycerol at –8 °C. ASW was prepared from Tropical Marin marine salt (33.33 g marine salt, 1 L deionized water, pH 8.2). Experimental stock cultures were maintained on ZoBell agar Petri dishes and were stored at 4 °C for up to 4 weeks. Bacterial pre-cultures were prepared from several colony-forming units (CFUs) in ZoBell agar Petri dishes suspended in 25 mL of liquid ZoBell medium for 24 h and 36 h at 18 °C with shaking (150 rpm) for *C. marina* and *M. hydrocarbonoclasticus*, respectively. Subcultures containing 50 mL of liquid ZoBell medium were prepared from the pre-cultures to obtain an OD_{600} of 0.1 and were grown for 6 h and 10 h, respectively, for *C. marina* and *M. hydrocarbonoclasticus* at 18 °C with shaking (150 rpm).

Bacterial Adhesion by the Standard Method: See Figure S6, Supporting Information. Bacterial subcultures in the logarithmic phase were centrifuged (1 min, 8000 rpm), and the pellets were washed with filtered ASW and centrifuged. The pellets were re-suspended in filtered ASW and if necessary diluted with filtered ASW in order to obtain an OD_{600} of 0.1, corresponding to a concentration of 4×10^{-7} cells/mL. The concentration of the bacteria was determined by flow cytometry. The bacterial suspension was then used immediately for bacterial adhesion assays. The SAMs on gold (three replicates for each SAMs) were placed into individual compartments of polystyrene four-compartment plates ("QuadriPerm" dishes, Greiner Bio-One Ltd.), and 10 mL of bacterial suspension was added to fully immerse the SAMs. An additional slide was immersed in ASW only to check for possible contamination of the ASW. The dishes were placed on a rotary shaker at room temperature for 1 h at 50 rpm. The bacterial suspensions were then removed and 10 mL of filtered ASW was added for 1 min at 50 rpm to remove any suspended cells. After the removal of filtered ASW, 10 mL of a 2.5% solution of glutaraldehyde in ASW was added for 20 min at room temperature to fix adhered bacterial cells. SAMs were then rinsed once with 10 mL of Milli-Q H_2O/ASW (v/v) before being dried overnight at room temperature. Adhered bacterial cells were observed by staining with 5 µM SYTO13 (Invitrogen, Molecular Probes) (excitation and emission wavelengths: 488 and 509 nm, respectively), and covered with a glass coverslip (22 mm × 22 mm, VWR International). Slides were then immediately removed from the light for 10 min, before observation. The density of bacterial cells was determined using an AxioVision 4 image analysis system attached to a Zeiss epifluorescence microscope and a video camera. A total of 30 fields of view were counted for each of the three SAM replicates.

Bacterial Adhesion Measurements by SPR: All SPR measurements were performed on a Reichert SR7000DC dual channel spectrometer (Buffalo, NY, USA) at 25 °C. A two-channel flow cell with two independent parallel flow channels was used to carry out the bioadhesion experiments. A gold-coated SPR chip, derivatized with SAMs, was deposited on the base of the prism using index-matching oil. After a baseline signal was established by allowing degassed ASW to flow at a rate of 100 µL min^{-1} through the sensor, a diluted prepared suspension of bacteria in filtered ASW (OD_{600} = 1) was allowed to flow over the surface for 25 min at a flow rate of 25 µL min^{-1}, followed by washing with filtered ASW for 10 min to remove unbound or loosely attached bacteria.

EPS-Bacterial Adhesion Measurements by SPR: For EPS adhesion assays, a freshly prepared bacterial suspension in ASW (OD_{600} = 1) was filtered through a 0.22 µm membrane filter in order to remove all the bacterial cells. The procedure was repeated 10, 20, 60, and 120 min after preparation of the bacterial suspension. For each time point, OD_{600} was checked in order to confirm that it was constant and that cells were not dividing in suspension during the whole experiment time. The filtrate was allowed to flow over the surface for 25 min at a flow rate of 25 µL min^{-1}, after which, the surface was washed with filtered (0.22 µm) ASW for 10 min to remove unbound or loosely attached EPS components. For the EPS adhesion assays, EPS deposition for 25 min at a flow rate of 25 µL min^{-1} was immediately followed by the injection of a freshly prepared bacterial suspension, after which the surface was washed with filtered ASW for 10 min to remove unbound or weakly attached bacteria.

Supporting Information

Supporting Information is available from the Wiley Online Library or from the author.

Acknowledgements

The work was funded by the European Community Framework Programme 7, SEACOAT (Surface Engineering for Antifouling), under Grant Agreement number 237997. This research was also supported through Birmingham Science City: Innovative Uses for Advanced Materials in the Modern World (West Midlands Centre for Advanced Materials Project 2), supported by Advantage West Midlands (AWM) and part funded by the European Regional Development Fund (ERDF).

Received: December 19, 2011
Revised: February 29, 2012
Published online: May 21, 2012

[1] *Biofilms, Infection, and Antimicrobial Therapy* (Eds: J. L. Pace, M. E. Rupp, R. G. Finch), CRC, Boca Raton FL **2006**.
[2] J. D. Bryers, *Colloids Surf. B* **1994**, *2*, 9.
[3] R. G. Chapman, E. Ostuni, M. N. Liang, G. Meluleni, E. Kim, L. Yan, G. Pier, H. S. Warren, G. M. Whitesides, *Langmuir* **2001**, *17*, 1225.
[4] M. Hermansson, *Colloids Surf. B* **1999**, *14*, 105.
[5] I. Ofek, H. S. Courtney, D. M. Schifferli, E. H. Beachey, *J. Clin. Microbiol.* **1986**, *24*, 512.
[6] E. M. Tuomola, S. J. Salminen, *Int. J. Food Microbiol.* **1998**, *41*, 45.
[7] A. G. Gristina, R. A. Jennings, P. T. Naylor, Q. N. Myrvik, L. X. Webb, *Antimicrob. Agents Chemother.* **1989**, *33*, 813.
[8] F. D'Souza, A. Bruin, R. Biersteker, G. Donnelly, J. Klijnstra, C. Rentrop, P. Willemsen, *J. Ind. Microbiol. Biotechnol.* **2009**, *9*, 0681.

[9] J. D. Durtschi, M. Erali, L. K. Bromley, M. G. Herrmann, C. A. Petti, R. E. Smith, K. V. Voelkerding, *J. Med. Microbiol.* **2005**, *54*, 843.
[10] S. Stafslien, J. Daniels, B. Chisholm, D. Christianson, *Biofouling* **2007**, *23*, 37.
[11] *Handbook of Bacterial Adhesion* (Eds: R. J. Friedman, Y. H. An), Humana Press, TotowaNJ **2010**, p. 260.
[12] *Drug Discovery and Evaluation: Pharmacological Assays*, *Vol. 1*, 3rd ed. (Ed: H. G. Vogel), Springer, Berlin **2008**, p. 120.
[13] a) C. L. Yeung, P. Iqbal, M. Allan, M. Lashkor, J. A. Preece, P. M. Mendes, *Adv. Funct. Mater.* **2010**, *20*, 2657; b) P. M. Mendes, K. L. Christman, P. Parthasarathy, E. Schopf, J. Ouyang, Y. Yang, J. A. Preece, H. D. Maynard, Y. Chen, J. F. Stoddart, *Bioconjugate Chem.* **2007**, *18*, 1919.
[14] A. D. Taylor, J. Ladd, J. Homola, S. Jiang, in *Principles of Bacterial Detection: Biosensors, Recognition Receptors and Microsystems* (Eds.: M. Zourob, S. Elwary, A. Turner), Springer, New York **2008**.
[15] B. K. Oh, W. Lee, W. H. Lee, J. W. Choi, *Biotechnol. Bioprocess Eng.* **2003**, *8*, 227.
[16] A. T. A. Jenkins, A. Buckling, M. McGhee, R. H. ffrench-Constant, *J. R. Soc. Interface* **2005**, *2*, 255.
[17] M. W. Oli, W. P. McArthur, L. J. Brady, *J. Microbiol. Methods* **2006**, *65*, 503.
[18] M. R. Pourshafie, B. I. Marklund, S. Ohlson, *J. Microbiol. Methods* **2004**, *58*, 313.
[19] A. Salminen, V. Loimaranta, J. A. F. Joosten, A. S. Khan, J. Hacker, R. J. Pieters, J. Finne, *J. Antimicrob. Chemother.* **2007**, *60*, 495.
[20] I. Lundstrom, *Biosens. Bioelectron.* **1994**, *9*, 725.
[21] a) J. N. Israelachvili, *Intermolecular and Surface Forces*, 3rd ed., (Ed: J. Israelachvili), Academic Press, Waltham MA **2011**; b) *Bacterial Adhesion: Molecular and Ecological Diversity* (Ed: M. Fletcher), Wiley, New York **1996**.
[22] G. Harkes, J. Feijen, J. Dankert, *Biomaterials* **1991**, *12*, 853.
[23] a) J. A. Lichter, M. T. Thompson, M. Delgadillo, T. Nishikawa, M. F. Rubner, K. J. Van Vliet, *Biomacromolecules* **2008**, *9*, 1571; b) A. Rosenhahn, S. Schilp, H. J. Kreuzer, M. Grunze, *Phys. Chem. Chem. Phys.* **2010**, *12*, 4275.
[24] G. P. Sheng, H. Q. Yu, X. Y. Li, *Biotechnol. Adv.* **2010**, *28*, 882.
[25] a) B. C. van der Aa, Y. F. Dufrêne, *Colloids Surf. B* **2002**, *23*, 173; b) I. Ofek, R. J. Doyle, *Bacterial Adhesion To Cells And Tissues*, Chapman & Hall, New York **1994**; c) R. M. Donlan, *Emerg. Infect. Diseases* **2002**, *8*, 881.
[26] B. Vu, M. Chen, R. J. Crawford, E. P. Ivanova, *Molecules* **2009**, *14*, 2535.
[27] L. Akesso, M. E. Pettitt, J. A. Callow, M. E. Callow, J. Stallard, D. Teer, C. Liu, S. Wang, Q. Zhao, F. D'Souza, P. R. Willemsen, G. T. Donnelly, C. Donik, A. Kocijan, M. Jenko, L. A. Jones, P. C. Guinaldo, *Biofouling* **2009**, *25*, 55.
[28] C. Shea, J. W. Nunley, J. C. Williamson, H. E. Smithsomerville, *Appl. Environ. Microbiol.* **1991**, *57*, 3107.
[29] a) P. V. Bhaskar, H. P. Grossart, N. B. Bhosle, M. Simon, *FEMS Microbiol. Ecol.* **2005**, *53*, 255; b) B. Klein, V. Grossi, P. Bouriat, P. Goulas, R. Grimaud, *Res. Microbiol.* **2008**, *159*, 137.
[30] a) Z. Dai, H. X. Ju, *Phys. Chem. Chem. Phys.* **2001**, *3*, 3769; b) L. A. Godínez, R. Castro, A. E. Kaifer, *Langmuir* **1996**, *12*, 5087; c) K. Hu, A. J. Bard, *Langmuir* **1997**, *13*, 5114; d) E. Kokkoli, C. F. Zukosk, *Langmuir* **2000**, *16*, 6029; e) T. R. Lee, R. I. Carey, H. A. Biebuyck, G. M. Whitesides, *Langmuir* **1994**, *10*, 741; f) R. Schweiss, P. B. Welzel, C. Werner, W. Knoll, *Langmuir* **2001**, *17*, 4304; g) K. Sugihara, K. Shimazu, *Langmuir* **2000**, *16*, 7101; h) H. S. White, J. D. Peterson, Q. Cui, K. J. Stevenson, *J. Phys. Chem. B* **1998**, *102*, 2930.
[31] a) J. M. Campin, A. Martins, F. Silva, *J. Phys. Chem. C* **2007**, *111*, 5351; b) D. J. Garrett, B. S. Flavel, J. G. Shapter, K. H. R. Baronian, A. J. Downard, *Langmuir* **2010**, *26*, 1848.
[32] K. Melzak, E. Ralph, E. Gizeli, *Langmuir* **2001**, *17*, 1594.
[33] a) P. Harder, M. Grunze, R. Dahint, G. M. Whitesides, P. E. Laibinis, *J. Phys. Chem. B* **1998**, *102*; b) Z. K. Zheng, M. L. Yang, Y. Q. Liu, B. L. Zhang, *Nanotechnology* **2006**, 5378.
[34] a) R. T. Thomas, J. E. Houston, R. M. Crooks, T. Kim, T. A. Michalske, *J. Am. Chem. Soc.* **1995**, *117*; b) Y. Chen, A. Nguyen, L. Niu, R. M. Corn, *Langmuir* **2009**, *25*, 5054.
[35] C. D. Bain, E. B. Troughton, Y. T. Tao, J. Evall, G. M. Whitesides, R. G. Nuzzo, *J. Am. Chem. Soc.* **1989**, *111*, 321.
[36] S. Schilp, A. Rosenhahn, M. E. Pettitt, J. Bowen, M. E. Callow, J. A. Callow, M. Grunze, *Langmuir* **2009**, *25*, 10077.
[37] J. Bowen, M. E. Pettitt, K. Kendall, G. J. Leggett, J. A. Preece, M. E. Callow, J. A. Callow, *J. R. Soc. Interface* **2007**, *4*, 473.
[38] M. Bogdanov, J. Xie, P. Heacock, W. Dowhan, *J. Cell Biol.* **2008**, *182*, 925.
[39] A. L. Cordeiro, M. Nitschke, A. Janke, R. Helbig, F. D'Souza, G. T. Donnelly, P. R. Willemsen, C. Werner, *Express Polym. Lett.* **2009**, *3*, 70.
[40] T. Ederth, T. Ekblad, M. E. Pettitt, S. L. Conlan, C.-X. Du, M. E. Callow, J. A. Callow, R. Mutton, A. S. Clare, F. D'Souza, G. Donnelly, A. Bruin, P. R. Willemsen, X. J. Su, S. Wang, Q. Zhao, M. Hederos, P. Konradsson, B. Liedberg, *ACS Appl. Mater. Interfaces* **2011**, *3*, 3890.
[41] S. Herrwerth, W. Eck, S. Reinhardt, M. Grunze, *J. Am. Chem. Soc.* **2003**, *125*, 9359.
[42] S. Schilp, A. Kueller, A. Rosenhahn, M. Grunze, M. E. Pettitt, M. E. Callow, J. A. Callow, *Biointerphases* **2007**, *2*, 143.
[43] E. Ostuni, R. G. Chapman, M. N. Liang, G. Meluleni, G. Pier, D. E. Ingber, G. M. Whitesides, *Langmuir* **2001**, *17*, 6336.
[44] H. Wang, S. F. Chen, L. Y. Li, S. Y. Jiang, *Langmuir* **2005**, *21*, 2633.
[45] a) M. J. Gauthier, B. Lafay, R. Christen, L. Fernandez, M. Acquaviva, P. Bonin, J. C. Bertrand, *Int. J. Syst. Evol. Microbiol.* **1992**, *42*, 568; b) M. C. Marquez, A. Ventosa, *Int. J. Syst. Evol. Microbiol.* **2005**, *55*, 1349.